

# STALL SIMULATION OF FLOW AROUND AN AIRFOIL USING LES MODEL AND COMPARISON OF RANS MODELS AT LOW ANGLES OF ATTACK

**Farshad Rezaei**

*M.Sc.Student, Ferdowsi University of Mashhad  
Farshad\_r585@yahoo.com*

**Ehsan Roohi**

*Assistant professor, Ferdowsi University of  
Mashhad  
e.roohi@um.ac.ir*

**Mahmoud Pasandideh-Fard**

*Associate professor, Ferdowsi University of Mashhad  
Fard\_m@um.ac.ir*

## **Abstract**

*In this paper, the influence of turbulence modeling, Reynolds number and stall condition on the fluid numerical solution over NACA0012 airfoil is studied by using the OpenFOAM package. Large-eddy simulation (LES) turbulence model is used to simulate flow at a high angle of attack in near-stall or stall condition. Some vortexes are formed and caused to appear a fluctuation behavior of pressure distribution on the upper surface of the airfoil. Three RANS turbulence models, i.e.,  $K-\omega$  SST,  $K-\varepsilon$  and RNG  $K-\varepsilon$  are used at low angles of attack than stall condition and lift/drag coefficients of them are compared. Among different turbulence models, the best result for lift coefficient is obtained once  $K-\omega$  SST turbulence model is used and the best drag coefficient is obtained by RNG  $K-\varepsilon$  turbulence model.  $K-\omega$  SST turbulence model predicted the beginning of stall condition accurately whereas two other models were not able to predict it. The effects of Reynolds number on the lift coefficient have been investigated. It is observed that by increasing Reynolds number at constant Mach number the lift coefficient is increased and stall phenomena is happened at a higher angle of attack.*

**Key words:** Turbulence models- Stall- NACA0012- OpenFOAM- LES- Reynolds number- Mach number.

## **1. Introduction**

CFD simulation is becoming one of the most important parts of aerodynamic and fluid mechanics industries. Almost all aerodynamic cases that exist in our world have a connection with fluid dynamics. For the analysis of moving cases (or flow around objects) in CFD toolboxes, there exist some hypothetical models for turbulent simulation.

Dynamic stall is an unsteady instability typically associated with flow separation. The stall vortex is formed around its leading edge and travels along the airfoil surface as it grows, and finally separates from the airfoil surface near the trailing edge. Instability of dynamic stall grows with flow separation and eventually prevents the wing's ability to create lift toward the dynamic stall. Stall flow simulation has many difficulties by using Reynolds-averaged

Navier-Stokes (RANS) methods due to unsteady vortical flows. RANS methods intend to model the large scale eddies using a universal model. Large scale turbulence is affected by the flow geometry and boundary conditions and a universal model does not exist. Large Eddy Simulation (LES) is promising to overcome the disadvantages of the RANS model. In LES, the governing equations are spatially filtered on the scale of the numerical grid. The large energy containing scales are directly simulated, and the small scale eddies, which are generally more homogeneous and universal, are modeled. The large eddies are strongly affected by the flow field geometry boundaries. Therefore the direct computation of the large eddies by LES is more accurate than the modeling of the large eddies by RANS. Ladson [1] experimentally investigated the low-speed aerodynamic characteristics of the NACA 0012 airfoil. His results showed that changes in Reynolds number affect lift-curve slope and maximum lift coefficient. Moreau et al. [2] performed LES of the trailing edge flow and noise of a NACA0012 airfoil near stall condition. Dahlstrom [3] concerned the efforts of conducting a Large Eddy Simulation around an airfoil in his thesis. He had found that the treatment of the laminar region has a major effect on the turbulent boundary layer further downstream. Martinat et al. [4] provided a study of the NACA0012 dynamic stall at Reynolds number  $10^5$  and  $10^6$  by means of two- and three-dimensional numerical simulations and the turbulence effect on the dynamic stall is also studied by statistical modeling. He concluded that standard URANS turbulence modeling has shown a quite dissipative character that attenuates the instabilities and the vortex structures related to the dynamic stall. Wang et al. [5] presented a 2D computational investigating on the dynamic stall phenomenon associated with unsteady flow around the NACA0012 airfoil at low Reynolds number ( $Re_c \approx 10^5$ ). He concluded that the CFD prediction captures well the vortex-shedding predominated flow structure which is experimentally obtained and the results quantitatively agree well with the experimental data, except when the blade is at a very high angle of attack. IM et al. [6] performed DES (Detached Eddy Simulation) and DDES (Delayed Detached Eddy Simulation) of NACA0012 airfoil near stall condition. They showed that DDES and DES predicted the drag coefficient accurately, while URANS (unsteady Reynolds-averaged Navier-Stokes) overpredicted the drag by 33.6%. Different researchers employed OpenFOAM for aerodynamic proposes. For example, Richez et al. [7] investigated the course of events leading to stall just before its occurrence and LES of the flow around an airfoil profile at high angle of attack had been achieved. Analysis of his results underlines the strong effect of the laminar separation bubble (LSB) structure on the whole downstream flow and, in particular, on the length of turbulent separation at the trailing edge. He also employed a zonal RANS/LES hybrid method and showed there is a good agreement with the LES in the separated flow. According to our best knowledge, there is not any detailed investigation of separated flow field around NACA0012 using OpenFOAM package.

RANS turbulence models are so popular to simulate flow field around an airfoil at low angles of attack. Yilbus et al. [8] tested Numerical simulation of the flow field around a cascade of NACA 0012 airfoils-effects of solidity and stagger. He had found that solidity increases the incidence at which maximum lift is obtained and, in this case, a slight increase in drag occurs. Council et al. [9] Validated the URANS shear stress transport  $\gamma$ -Re model for low-Reynolds-number external aerodynamics. In view of the results which they obtained, the proposed model is deemed appropriate for modeling low-Reynolds-number external aerodynamics and provides a framework for future studies for the better understanding of this complex flow regime. Mompean [10] examined numerical simulation of a turbulent flow near

a right-angled corner using the non-linear model with RNG K- $\epsilon$  equations. He showed that The predictions obtained with the RNG K- $\epsilon$  model show small improvements when compared with the standard K- $\epsilon$ . Dahlstrom and Davidson [11] used Large Eddy Simulation (LES) to calculate the flow around the Aerospatiale A-profile airfoil at an angle of attack of 13.3 degree at Reynolds number of  $2.1 \times 10^6$ . The method used was an incompressible implicit second-order finite volume method with a collocated grid. Davidson [12] used a second moment Reynolds Stress Transport Model (RSTM) for computing the flow around a two dimensional airfoil. An incompressible SIMPLE code was used, employing a non- staggered grid arrangement.

Accurate numerical simulation of flow field over external geometries needs considering different points such as employing suitable grid size (especially in the boundary layer), applying accurate discretization model (specifically near stall condition), and consideration of suitable turbulence transition. In this paper, we numerically examined incompressible flow around NACA 0012 airfoil using the open source CFD package of OpenFOAM. Within the framework of OpenFOAM, we have used *pisoFoam* solver for LES and *simpleFoam* solver for the RANS cases. The PISO (Pressure Implicit with Splitting of Operators) is an efficient method to solve the Navier-Stokes equations in unsteady incompressible problems. This algorithm is iterative procedures for solving equations for velocity and pressure, PISO being used for transient problems. *SimpleFoam* is a pressure-based solver which solves the momentum equation with under relaxation factors and then iteratively applies a pressure correctors equation based on the conservation of mass to evaluate the velocity and pressure fields. The turbulence model equations are solved after the velocity and pressure are computed at each time step, and an iterative update is performed on the later fields before a consecutive step is performed. SIMPLE algorithm was used for pressure-velocity coupling.

The numerical simulation reported in the present work has been conducted using OpenFOAM 2.1.0 code. OpenFoam has attracted much attention recently because it is a sustainable open source code designed for a wide range of CFD applications. It is a C++ toolbox based on object oriented programming [13]. OpenFOAM is released under the GPL [14-15] and it consists of enormous groups of libraries for different mathematical, numerical and physical models. Linking the mathematical/numerical tools with the physical models in a main C++ function produces different solvers and utilities. OpenFOAM allows the users freely choose among a wide range of numerical discretization and interpolation schemes.

## 2. Turbulence Models

### 2.1. LES Model

Large eddy simulation (LES) is based on computing the large, energy-containing structures that are resolved on the computational grid, whereas the smaller, more isotropic, sub-grid structures are modeled [16]. In contrast to RANS approaches, which are based on solving for an ensemble average of the flow properties, LES naturally and consistently allows for medium to small scale, transient flow structures. Starting from the incompressible Navier-Stokes (NS) equations, the governing flow equations consists of the balance equations of mass and momentum,

$$\begin{aligned} \partial_t(\rho v) + \nabla \cdot (\rho v \times v) &= -\nabla p + \nabla \cdot s, \\ \partial_t \rho + \nabla \cdot (\rho v) &= 0 \end{aligned} \tag{1}$$

where  $v$  is the velocity,  $p$  is the pressure,  $s = 2\mu D$  is the viscous stress tensor, where the rate-of-strain tensor is expressed as

$$D = \frac{1}{2}(\nabla v + \nabla v^T) \quad (2)$$

where  $\mu$  is the viscosity. The LES equations are theoretically derived, following e.g. Sagaut [17] from Eq. (1). In ordinary LES, all variables, i.e.,  $f$ , are split into grid scale (GS) and subgrid scale (SGS) components,  $f = \bar{f} + f'$ , where  $\bar{f} = G * f$  is the GS component,  $G = G(X, \Delta)$  is the filter function, and  $\Delta = \Delta(\mathbf{x})$  is the filter width. The LES equations result from convolving the NS with  $G$ , viz.,

$$\begin{aligned} \partial_t(\rho \bar{v}) + \nabla \cdot (\rho \bar{v} \times \bar{v}) &= -\nabla \bar{p} + \nabla \cdot (\bar{s} - B), \\ \partial_t \rho + \nabla \cdot (\rho \bar{v}) &= 0 \end{aligned} \quad (3)$$

where over-bar denotes filtered quantity. Equation (3) introduces one new term when compared to the unfiltered Eq. (1): the unresolved transport term  $B$ , which is the sub grid stress tensor. Following Bensow and Fureby [18],  $B$  can be exactly decomposed as

$$B = \rho \cdot \left( \overline{\bar{v} \times \bar{v}} - \bar{\bar{v}} \times \bar{\bar{v}} + \tilde{B} \right) \quad (4)$$

where now only  $\tilde{B}$  needs to be modeled. The most common subgrid modeling approaches utilizes an eddy or subgrid viscosity,  $\nu_{SGS}$ , similar to the turbulent viscosity approach in RANS, where  $\nu_{SGS}$  can be computed in a wide variety of methods. In eddy-viscosity models often,

$$B = \frac{2}{3} \bar{\rho} k l - 2 \mu_k \tilde{D}_D \quad (5)$$

where  $k$  is the SGS kinetic energy,  $\mu_k$  the SGS eddy viscosity, and  $D_D$  the SGS eddy diffusivity. In the current study, subgrid scale terms are modeled using “one equation eddy viscosity” model. In order to obtain  $k$ , one-equation eddy-viscosity model (OEEVM) uses the following equation:

$$\sigma_t(\bar{\rho} k) + \nabla \cdot (\bar{\rho} k \tilde{V}) = -B \cdot (\mu \nabla k) + \bar{\rho} \varepsilon \quad (6)$$

Where

$$\varepsilon = C_\varepsilon k^{3/2} / \Delta$$

$$\mu_k = C_k \bar{\rho} \Delta \sqrt{k} \quad (7)$$

## 2.2. RANS Models

The K-epsilon model is one of the most common turbulence models, although it just doesn't perform well in cases of large adverse pressure gradients [19]. It is a two equation model, which means, it includes two extra transport equations to represent the turbulent properties of the flow. This allows a two equation model to account for history effects like convection and diffusion of turbulent energy. The first transported variable is turbulent kinetic energy,  $k$ . The second transported variable in this case is the turbulent dissipation,  $\epsilon$ . It is the variable that determines the scale of the turbulence, whereas the first variable,  $k$ , determines the energy in the turbulence. There are two major formulations of K-epsilon models [20,21]. That of Launder and Sharma is typically called the "Standard" K-epsilon Model. The original impetus for the K-epsilon model was to improve the mixing-length model, as well as to find an alternative to algebraically prescribing turbulent length scales in moderate to high complexity flows. The K-epsilon model has been shown to be useful for free-shear layer flows with relatively small pressure gradients. Similarly, for wall-bounded and internal flows, the model gives good results only in cases where mean pressure gradients are small; accuracy is reduced for flows containing large adverse pressure gradients.

The RNG model was developed using Re-Normalization Group (RNG) methods by to renormalize the Navier-Stokes equations, to account for the effects of smaller scales of motion [22]. In the standard k-epsilon model the eddy viscosity is determined from a single turbulence length scale, so the calculated turbulent diffusion is that which occurs only at the specified scale, whereas in reality all scales of motion will contribute to the turbulent diffusion. The RNG approach, which is a mathematical technique that can be used to derive a turbulence model similar to the k-epsilon, results in a modified form of the epsilon equation which attempts to account for the different scales of motion through changes to the production term.

The SST k- $\omega$  turbulence model [23] is a two equation eddy-viscosity model which has become very popular. The shear stress transport (SST) formulation combines the best of two worlds. The use of a k- $\omega$  formulation in the inner parts of the boundary layer makes the model directly usable all the way down to the wall through the viscous sub-layer, hence the SST k- $\omega$  model can be used as a Low-Re turbulence model without any extra damping functions. The SST formulation also switches to a k- $\epsilon$  behavior in the free-stream and thereby avoids the common k- $\omega$  problem that the model is too sensitive to the inlet free-stream turbulence properties. Authors who use the SST k- $\omega$  model often merit it for its good behavior in adverse pressure gradients and separating flow. The SST k- $\omega$  model does produce a bit too large turbulence levels in regions with large normal strain, like stagnation regions and regions with strong acceleration. This tendency is much less pronounced than with a normal k- $\epsilon$  model though.

## 3. Results and Discussion

### 3.1. LES Model

The computational domain and applied boundary condition is schematically shown in figure 1. The flow field around NACA 0012 airfoil at velocity of 68 m/s and Mach number of 0.2 and Reynolds number of  $3.97 \times 10^6$  for simulating stall condition at angle of attack  $18^\circ$  is considered. The chord length of the airfoil is 1 m and the employed Turbulence model is LES

using one equation eddy for subgrid model. Different meshes had been produced and the accuracy of numerical solution is investigated. Meshes information are given in table 1. Lift coefficients for all three meshes are shown in figure 2. Ladson's experimental results [1] are used for comparing the current numerical simulation and experimental data. Figure 2 shows that the best result is given by grid 3 which is close to Ladson's experimental data.

Table 1: Meshes information

Mesh Name	Number of points on the airfoil	Thickness of first B.L cell (mm)
Grid 1	860	0.04
Grid 2	960	0.02
Grid 3	960	0.01

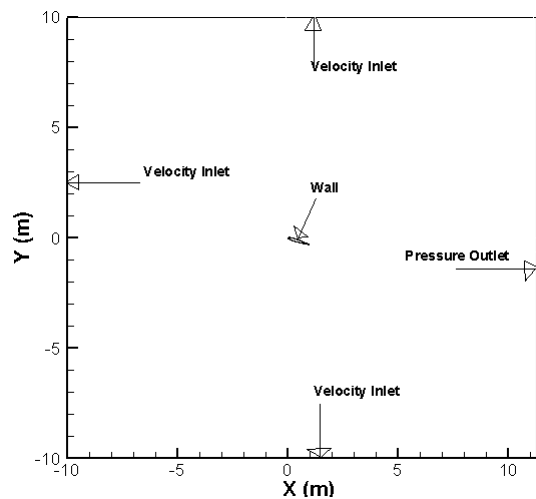


Figure 1: Computational domain and applied boundary conditions around NACA 0012 airfoil

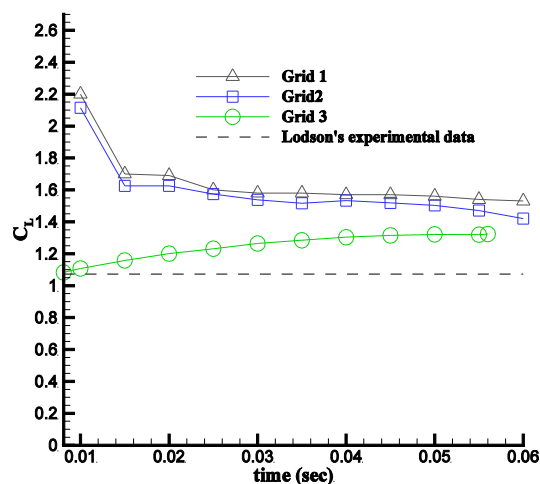


Figure 2:  $C_L$  variation vs. time for different grids at angle of attack  $18^\circ$  using LES

Lift and Drag coefficient for grid 3 are shown in figure 3. It is observed that there is a good agreement with the experimental data.

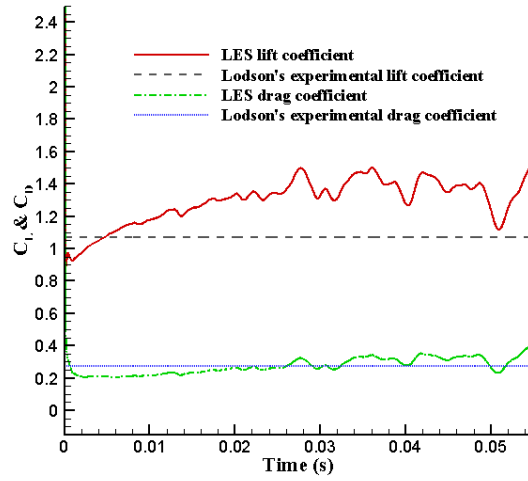


Figure 3:  $C_L$  &  $C_D$  Variations vs. time from the current LES numerical work compared with the numerical data of Ref. [1]

It is observed from figure 3 that at initial times (before  $t=0.005$  second (5 mm second)) lift and drag coefficients are so close to experimental data, because at the mentioned times, vortices have not been formed and wall pressure coefficient is so smooth. After that, vortices are formed gradually and affect the wall pressure coefficient. It is clear that after  $t=0.025$  (ms) lift and drag coefficients have a fluctuation behavior and this is nearly consonant with the physical fact. So the average of lift and drag coefficients have to be computed.

Figure 4 shows velocity contours at four different times and their appropriate wall pressure coefficients. It is observed that by the time going forward, some vortices are appeared and moved in line with the upper surface of the airfoil, and usually separated along the way of upper surface. The process of formation and separation of vortices is repeatable.

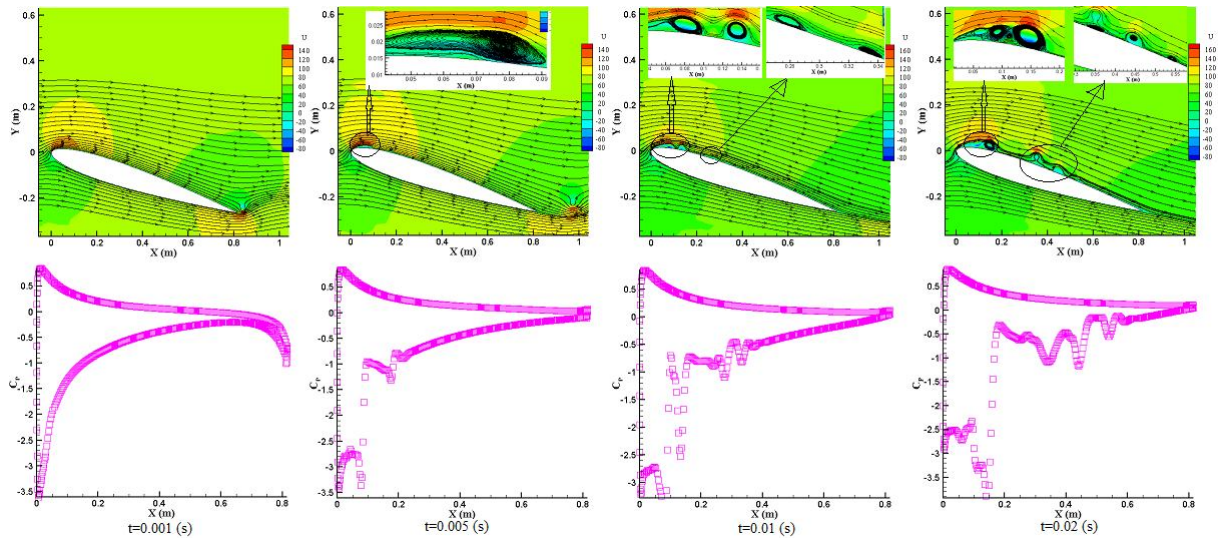


Figure 4: Velocity contours at 4 different times with their wall pressure coefficients at  $Ma=0.2$  and  $Re=3.97 \times 10^6$  using LES

Formation and separation of vortices are unsteady, but by increasing the time, there are always some vortices on the upper surface of the airfoil, figure 5 shows this issue. It is observed that vortices are cause to have a fluctuation behavior of pressure distribution on the

upper surface of airfoil. So, the pressure center and other aerodynamic forces center are moved to the leading edge and fluctuated in the first half of chord. This subject is causing the airfoil to be unstable and has serious implications in terms of achievable performance, which needs to be predicted accurately as soon as possible in the airfoil design cycle.

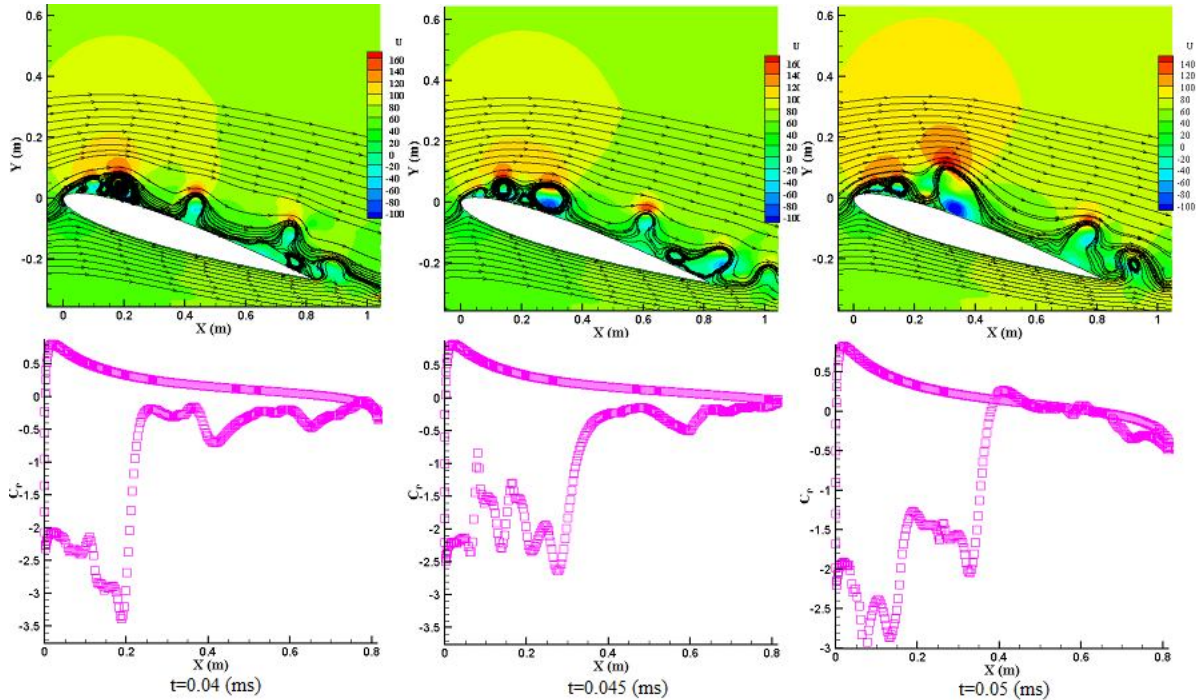


Figure 5: Effect of vortices on the wall pressure coefficient distribution at  $Ma=0.2$  and  $Re=3.97 \times 10^6$

### 3.2. RANS Models

According to the results obtained from using three different turbulence models i.e.,  $K-\omega$  SST,  $K-\epsilon$  and RNG  $K-\epsilon$ , the  $K-\omega$  SST turbulence model gave us the best lift coefficient in compare of two other turbulence models. Figure 6 Shows lift and drag coefficients for different turbulence models in compare to Ladson experimental data [1]. These results are obtained for  $Ma=0.15$  and  $Re=2 \times 10^6$ . Among Three different turbulence models which are used in this work, RNG  $K-\epsilon$  predicted drag coefficient more accurate in compare to two other models.

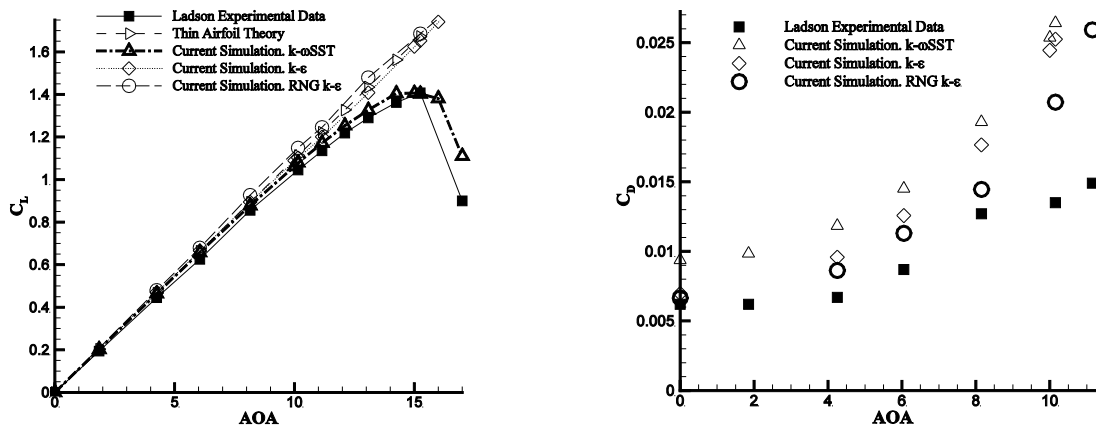


Figure 6:  $C_L$  and  $C_D$  variations vs. angle of attack at  $Ma=0.15$  and  $Re=2 \times 10^6$  from the current numerical work by using RANS models compared with the numerical data of Ref. [1]

Dependency of flow solution to the Reynolds number at the constant Mach number has been examined. Figure 7 shows  $C_L$  variations at flow with  $Ma=0.15$  and three different Reynolds number using  $K-\omega$  SST turbulence model. The results are compared with Ladson experimental data [1] at  $Ma=0.15$  and  $Re=2 \times 10^6$ . It is realized that by increasing Reynolds number at constant Mach number, the lift slope is increased a little. This result has a good agreement with experimental data which are achieved by Ladson[1]. It is realized from figure 6 that stall phenomena is predicted well at flow with different Reynolds number using  $K-\omega$  SST turbulence model. Also, stall phenomena is occurred at a higher angle of attack by increasing Reynolds number.

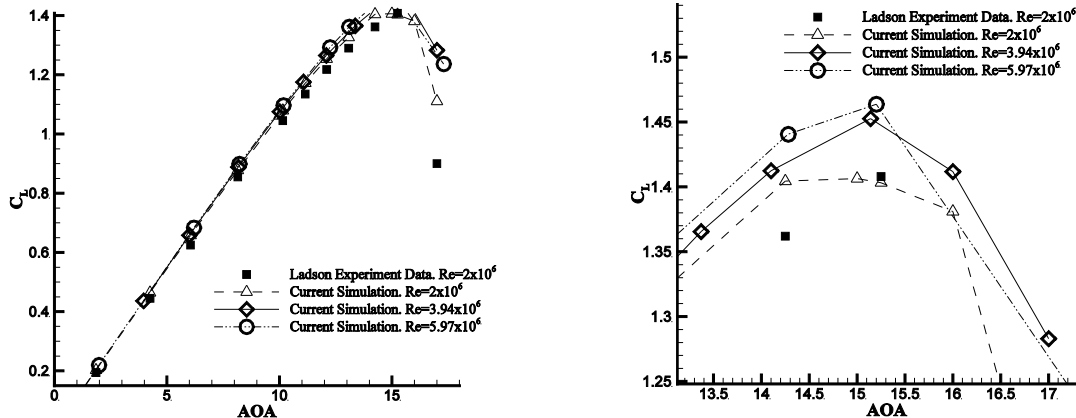


Figure 7:  $C_L$  variation vs. angle of attack at  $Ma=0.15$  and three different Reynolds number compared with the numerical data of Ref. [1]

#### 4. Conclusions

Large-eddy simulation of flow over a NACA0012 airfoil at high angle of attack in stall condition is investigated. Vortexes are appeared on the upper surface of airfoil and moved along the surface and separated. The influence of vortexes to have fluctuation behavior on wall pressure coefficient is investigated and it is realized that these vortexes cause to move aerodynamic forces center to the leading edge. The effects of turbulence modeling and Reynolds number on the numerical solution over the airfoil investigated. Three turbulence models, i.e.,  $K-\omega$  SST,  $K-\epsilon$  and RNG  $K-\epsilon$  are used. Among them, the best result for lift coefficient is obtained once  $K-\omega$  SST turbulence model is tried and the best drag coefficient is obtained by RNG  $K-\epsilon$  turbulence model.  $K-\omega$  SST turbulence model predicted near stall condition well whereas two other models were not able to predict it. The effects of Reynolds number on the lift coefficient have been investigated. It is realized that by increasing Reynolds number at constant Mach number the lift-curve slope is increased.

#### References

- [1] Ladson, C.H, effects of Independent Variation of Mach and Reynolds Numbers on the Low-Speed Aerodynamics Characteristics of the NACA0012 Airfoil Section, NASA TM 4074 report, (1988).
- [2] Moreau, S., Christophe, J. and Roger, M., Les of the trailing-edge flow and noise of a NACA0012 airfoil near stall, Proceeding of the summer program, Center for Turbulence Research,(2008).

- [3] Dahlstrom, S., Large Eddy Simulation of the Flow Around a High-Lift Airfoil , Master of Science Thesis, Chalmers University of Technology, (2003).
- [4] Martinat, G., Braza, M., Hoarau, Y. and Harran, G., Turbulence modeling of the flow past a pitching NACA0012 airfoil at  $10^5$  and  $10^6$  Reynolds number, Journal of Fluids and Structures 24, PP 1294-1303 (2008).
- [5] Wang. S., Ingham. D.B., Ma. L., Pourkashian. M. and Tao. Z., Numerical investigations on dynamic stall of low Reynolds number flow around oscillating airfoils, Computers & Fluids 39, PP 1529-1541 (2010).
- [6] IM, H.S. and Zha, G.C., Delayed Detached Eddy Simulation of a Stall Flow over NACA0012 Airfoil Using High Order Schemes AIAA-1297 (2011).
- [7] Richez, F., Mary, I., Gleize, V. and Basdevant, C., Near stall simulation of the flow around an airfoil using zonal RANS/LES coupling method, Computers & Fluids 37, PP 857-866 (2008).
- [8] Yilbus, B.S., Budair, M.O., and Naweed Ahmed. M., 1197. Numerical simulation of the flow field around a cascade of NACA 0012 airfoils-effects of solidity and stagger. Comput. Methods Appl. Mech. Engrg. 158,pp.143-154 (1998).
- [9] Council, J.N.N., and Goni Boulama. K., Validating the URANS shear stress transport  $\gamma$ -Re model for loe-Renolds-number external Aerodynamics, Int. J. Numer. Meth. Fluids (2012).
- [10] Mompean. G., Numerical simulation of a turbulent flow near a right-angled corner using the Speziale non-linear model with RNG K- $\epsilon$  equations, Computers & Fluids Vol. 27, No. 7, pp. 847-859, (1998).
- [11] Dahlstrom, S. and Davidson, L., "Large Eddy Simulation of the flow around an Airfoil" AIAA Aerospace Sciences Meeting and Exhibit 8-11, (2001).
- [12] Davidson, L., calculation of the flow around A-Airfoils Using an Incompressible Code Based on SIMPLE and two layer k- $\epsilon$  model, 42, AV. Gustave Coriolis 31057 Toulouse, France, Report TR/RE/92/73, (1991).
- [13] Tabor, H.G., Jask,H.,Furbey,C., A tensorial approach to computational continuum mechanics using object-oriented techniques, Compute. Phys. (6) (1998).
- [14] <http://www.openfoam.com>
- [15] OpenFOAM, OpenFoam user guide. (2011).
- [16] Roohi, E., Zahiri, A. P., Passandideh-Fard, M., Numerical Simulation of Cavitation around a Two-Dimensional Hydrofoil Using VOF Method and LES Turbulence Model, Applied Mathematical Modeling, In press, 2013, DOI: 10.1016/j.apm. (2012).
- [17] Sagaut T, P., Large Eddy Simulation for Incompressible Flows, Springer, New York, 3<sup>rd</sup>edition, (2006).
- [18] - Fureby, C., and Grinstein, F., Large Eddy Simulation of High-Reynolds Number Free and Wall-Bounded Flows, journal of Computational Physics, Vol.181, pp. 68–97, (2002).
- [19] Wilcox, David C , Turbulence Modeling for CFD. Second edition. Anaheim: DCW Industries. pp. 174, (1998).
- [20] Jones, W. P., and Launder, B. E., The Prediction of Laminarization with a Two-Equation Model of Turbulence, International Journal of Heat and Mass Transfer, vol. 15, pp. 301-314, (1972).
- [21] Launder, B. E., and Sharma, B. I., Application of the Energy Dissipation Model of Turbulence to the Calculation of Flow Near a Spinning Disc, Letters in Heat and Mass Transfer, vol. 1, no. 2, pp. 131-138, (1974).
- [22] Yakhot, V., Orszag, S.A., Thangam, S., Gatski, T.B. & Speziale, C.G., Development of turbulence models for shear flows by a double expansion technique, Physics of Fluids A, Vol. 4, No. 7, pp1510-1520, (1992).
- [23] Menter, F. R., Zonal Two Equation k- $\omega$  Turbulence Models for Aerodynamic Flows, AIAA Paper, 93-2906, (1993).